THE JOURNAL OF PHYSICAL CHEMISTRY Letters

Letter

pubs.acs.org/JPCL

Molecular Dipole-Driven Electronic Structure Modifications of DNA/RNA Nucleobases on Graphene

Yuefeng Yin,[†] Jiri Cervenka,*[,‡] and Nikhil V. Medhekar*[,†]

[†]Department of Materials Science and Engineering, Monash University, Wellington Road, Clayton, Victoria 3800, Australia

[‡]Department of Thin Films and Nanostructures, Institute of Physics ASCR, v. v. i., Prague 182 21, Czech Republic

Supporting Information

ABSTRACT: The emergence of graphene in recent years provides exciting avenues for achieving fast, reliable DNA/RNA sensing and sequencing. Here we explore the possibility of enhancing electronic fingerprints of nucleobases adsorbed on graphene by tuning the surface coverage and modifying molecular dipoles using first-principles calculations. We demonstrate that intermolecular interactions have a strong influence on the adsorption geometry and the electronic structure of the nucleobases, resulting in tilted configurations and a considerable modification of their electronic fingerprints in graphene. Our analysis reveals that the molecular dipole of the nucleobase molecules plays a dominant role in the electronic structure of graphene−nucleobase systems, inducing significant changes in the work functions and energy level alignments at the interface. These results highlight tunable control of the measured molecular signals in graphene by optimizing the surface contact between nucleobases and graphene. Our findings have important implications for identification and understanding of molecular fingerprints of DNA/RNA nucleobases in graphene-based sensing and sequencing methods.

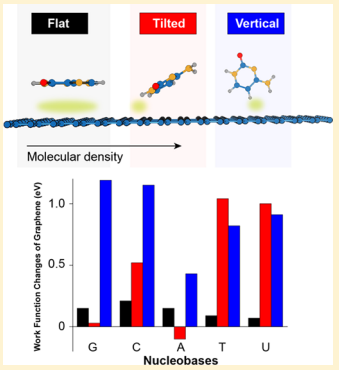

The ability to detect biologically important molecules (such as DNA and RNA) in a sensitive, selective, and cost-effective manner is playing an increasingly important role in numerous fields such as medicine, biology, forensics, and technology.[1−6] Graphene-based biosensors have attracted extensive attention in recent years as they exhibit a high potential of providing fast, label-free, and ultrasensitive detection of biomolecules and nanomaterials.[7−12] Graphene, owing to its unique structure and electronic properties, offers many new opportunities for detection and quantification of nucleic acid sequences in DNA and RNA as well as in whole DNA strand sensing.[3,13−17] Recently, numerous approaches have been proposed to achieve label-free real-time molecule-specific detection of DNA and RNA nucleobases with graphene.[18−26] Among these, electronic detection methods using graphene nanodevices and nanopore-based architectures are the most promising.[3] Despite their potential, there are still many issues that need to be solved before these approaches can be implemented in real applications, particularly due to a lack of fundamental understanding of graphene−nucleobase interactions and the origin of measured molecular fingerprints.

From an experimental perspective, detection of DNA using graphene-based electronic sensors has been realized by measuring conductance changes in graphene or a shift of the Dirac point as a function of gate voltage in graphene field effect transistors (FETs).[27−31] Both n-type[27−29] and p-type[30,31] doping of graphene caused by adsorption of DNA have been reported. The experimental conditions seem to have a significant influence as reported by Lin et al.,[29] showing both p- and n-type doping of graphene in liquids but only n-type doping in vacuum. Adsorption of layers of individual DNA nucleobases on graphene FETs in vacuum has been found to exhibit complex coverage-dependent behavior with n-type doping for cytosine and thymine, p-type doping for adenine, and both n-type and p-type doping for guanine.[32] These observations present a clear challenge on how to programmably control the electronic signals from graphene−DNA interactions and achieve distinct single-base sensing.

Previous theoretical studies have shown that the interaction of DNA/RNA with graphene is dominated by the weak noncovalent $\pi-\pi$ interaction between nucleobases and graphene.[33−42] The weak nature of this interaction indicates that the electronic structure of the graphene−nucleobase system can be readily tuned by altering surface contact between the substrate and the adsorbate. A recent experimental study has shown that tilted adsorption of DNA nucleobases on graphene is possible in thin submonolayer layers and can result in both n- and p-type doping of graphene depending on the coverage.[32] This finding offers a tantalizing possibility for the role of adsorption geometry and molecular dipole moments in modifying the electronic signals of nucleobases. A novel theoretical model is therefore needed to explore new pathways for enhancing DNA/RNA base sensing based on molecular dipoles.

Here, we report on a systematic electronic structure study of nucleic acid bases on graphene as a function of molecular

Received: May 23, 2017
Accepted: June 19, 2017
Published: June 19, 2017

DOI: 10.1021/acs.jpclett.7b01283
J. Phys. Chem. Lett. 2017, 8, 3087−3094

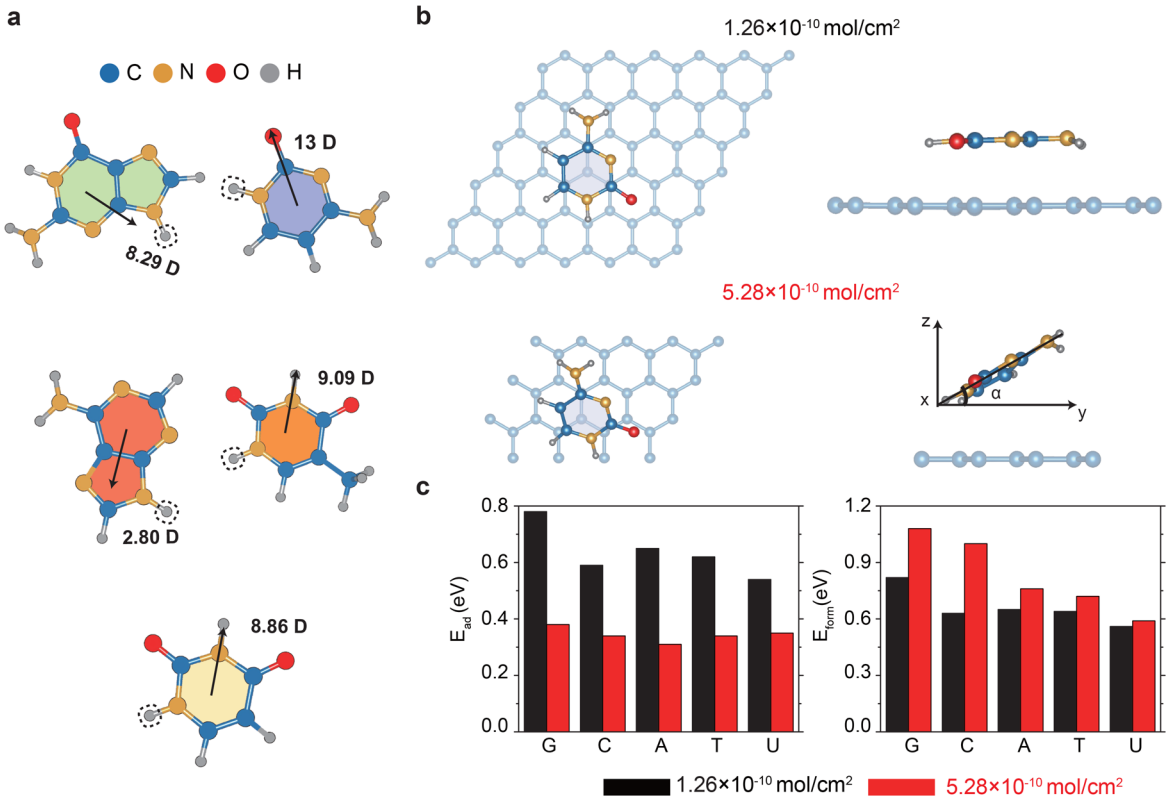

Figure 1. Adsorption geometry and energies of nucleobases on graphene. (a) Atomic structure of isolated nucleobases showing the direction and magnitude of their in-plane dipole moments. (b) Top and side views of optimized adsorption configurations of the nucleobases on graphene at low (1.26×10^{-10} mol/cm^2) and high (5.28×10^{-10} mol/cm^2) molecular concentrations. (c) Adsorption energy (E_{ad}) and formation energy (E_{form}) of the physisorbed nucleobases at different molecular concentrations.

orientation and surface coverage using density functional theory with van der Waals corrections. We demonstrate that the adsorption geometry and the electronic structure of DNA/RNA nucleobases on graphene is strongly influenced by intermolecular interactions, leading to a tilt of the nucleobases on graphene at high molecular densities. As the nucleobases possess strong in-plane dipole moments (Figure 1a), their tilt causes significant changes of the electronic structure of the whole graphene−nucleobase system. We analyze how this affects the molecule-specific features in the local density of states close to the Fermi level, HOMO−LUMO energy levels, and the work function of graphene. We identify that the in-plane dipole moments play a dominant role in altering the electronic structure of graphene and lead to both p- and n-type doping of graphene depending on the direction of the *z*-component of the interface dipole moment. Using this mechanism, we suggest a new strategy for enhancing the measured signals of DNA/RNA nucleobases adsorbed on graphene by using vertically aligned nucleobases. Our results provide a new understanding of interfacial interactions and molecule-specific signatures of DNA/RNA nucleobases on graphene.

The optimized geometry and the electronic structure of the adsorbed nucleobases on graphene are obtained using first-principles density functional theory as implemented in the Vienna ab initio simulation package (VASP). The Perdew−Burke−Ernzerhof (PBE) form of the generalized gradient approximation (GGA) is used to describe electron exchange and correlation.[43] The kinetic energy cutoff for the plane-wave basis set is set to 600 eV. A semiempirical functional developed by Grimme (DFT-D2)[11,44] is used to describe dispersion forces.[38] We have also confirmed the consistency of our results by using different approaches to treat dispersion forces; see Figure S1 in the Supporting Information. We study a series of molecular concentrations from isolated molecules to a close-packed monolayer coverage similar to that in experiments, which is in the range of 1.26×10^{-10}−5.28×10^{-10} mol/cm^2. To achieve this, we consider hexagonal unit cells of various sizes with each unit cell containing a nucleobase molecule adsorbed on a free-standing graphene.[45] Here, we present concentrations of 1.26×10^{-10} and 5.28×10^{-10} mol/cm^2 as representatives of low and high molecular concentrations, respectively, as shown in Figure 1b. Other molecular concentrations considered in this study are shown in the Supporting Information (Figures S2 and S3, Tables S1 and S2). All structures were fully relaxed until the ionic forces were smaller than 0.01 eV/Å. For accurate calculations of the electronic structures, we used $12 \times 12 \times 1$ and $20 \times 30 \times 1$ Γ-centered grids for sampling the Brillouin zone at low and high molecular concentrations, respectively.

Figure 1b shows that increasing the molecular concentration has a significant effect on the molecular geometry and adsorption energetics of adsorbed DNA/RNA nucleobases on graphene. The most significant geometry change is found in the tilt angle of the nucleobases, α, defined as the rotation angle of the molecular plane around the x axis with respect to the graphene surface (xy plane). The tilt angle of isolated molecules at low molecular concentration (1.26×10^{-10} mol/cm^2) is close to zero, similar to previous theoretical calculations.[34] The tilt angle becomes significant at high molecular concentrations (see

DOI: 10.1021/acs.jpclett.7b01283
J. Phys. Chem. Lett. 2017, 8, 3087−3094

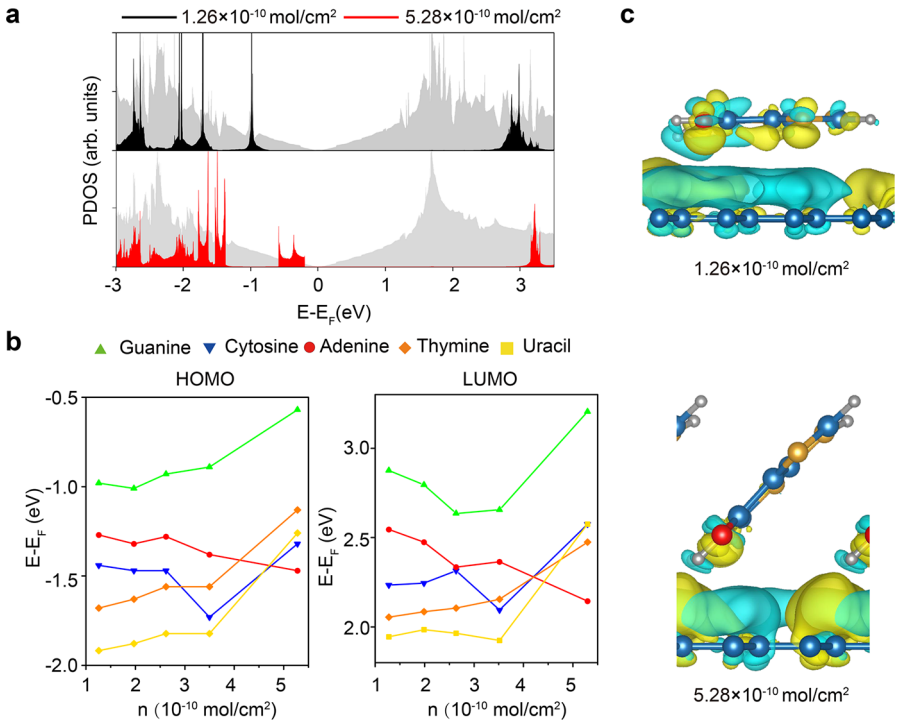

Figure 2. Electronic structure of nucleobases on graphene. (a) PDOS of guanine upon adsorption on graphene at molecular concentrations of 1.26 × 10^{-10} (black) and 5.28 × 10^{-10} mol/cm^2 (red). PDOS of graphene upon adsorption is shown in gray. (b) HOMO and LUMO peaks of the nucleobases as a function of molecular concentration. (c) Side views of the charge density difference of guanine on graphene at low and high molecular concentrations. The yellow (cyan) isosurface denotes charge accumulation (depletion). The isosurface level is ±0.002 e/Å^3.

Table S1), reaching 46°, 29°, 67°, 45°, and 38° for guanine, cytosine, adenine, thymine, and uracil, respectively, at 5.28 × 10^{-10} mol/cm^2. These values are close to the experimentally measured tilt angles of nucleobases on graphene using angle-resolved near edge X-ray adsorption fine structure (NEXAFS) measurements, which found α at around 40° for all nucleobases at a molecular coverage above 0.5 monolayer.[32]

To investigate the stability of the nucleobases physisorbed on graphene in different concentrations, we calculate the adsorption energy (E_{ad}) per nucleobase molecule defined as $E_{ad} = E_{gra} + E_{base} - E_{gra-base}$, where $E_{gra-base}$ is the total energy of the relaxed graphene−base system and E_{gra} and E_{base} are energies of the free-standing graphene and the nucleobase layer with the same density. We also calculate the formation energy (E_{form}) to quantify the thermodynamic stability of the graphene−base system with respect to the isolated states of its individual constituents as $E_{form} = E_{gra} + E_{iso-base} - E_{gra-base}$. The energy of an isolated nucleobase ($E_{iso-base}$) is defined as the energy of a nucleobase molecule in the gas phase. With this notation, positive adsorption and formation energies indicate thermodynamically favorable adsorption of a nucleobase on graphene.

It is clear from Figure 1c that at low molecular concentration, the adsorption energy follows the order G > A ≈ T > C > U, consistent with previous theoretical studies that suggest that the adsorption strength correlates with the molecular polarizability.[33,46,47] Figure 1c also shows that the adsorption energy is 0.2−0.4 eV higher at low molecular concentration of the nucleobases than at high concentration. This can be attributed to parallel $\pi-\pi$ stacking between graphene and nucleobases, which enables better contact between π orbitals of aromatic cores of the nucleobases and graphene. This observation agrees well with previous studies highlighting the effect of molecular geometry and indicates that the adsorption of tilted molecules can be significantly stabilized by increasing molecular concentration.[40,41] On the other hand, although the binding of the nucleobases on graphene becomes weaker at high molecular concentration, as the molecular plane of the nucleobases becomes tilted, intermolecular interactions further stabilize the system, resulting in the higher formation energy at high molecular concentration of 5.28 × 10^{-10} mol/cm^2. This shows that the formation of high-density tilted nucleobase layers is energetically more favorable than the isolated flat nucleobases on graphene, supporting recent experimental observations.[32,48]

The intermolecular binding energy of the nucleobases is estimated as the difference between the formation energy and the adsorption energy. The intermolecular binding energy at high molecular concentration follows the order G (0.75 eV) ≈ C (0.74 eV) > A (0.45 eV) > T (0.38 eV) > U (0.24 eV) and is expectedly negligible (~0.02 eV) at low molecular concentration. Detailed analysis of the intermolecular interactions shows that the stabilization of the tilted nucleobases on graphene originates mainly from the formation of hydrogen bonds between neighboring nucleobases.[49,50] These results demonstrate that the adsorption of nucleobase layers on graphene is driven by a subtle interplay between graphene−nucleobase and intermolecular interactions, and the resulting adsorption structure is expected to strongly depend on the exact conditions in experiments (e.g., surrounding molecules and ions).[29,32]

The changes in the adsorption geometry of nucleobases on graphene have a strong influence on the electronic structure of the whole system and the electronic fingerprints of DNA/RNA nucleobases on graphene, which are used for their identification.[18,34,40] Figure 2 demonstrates how the electronic

DOI: 10.1021/acs.jpclett.7b01283
J. Phys. Chem. Lett. 2017, 8, 3087−3094

structure of nucleobases on graphene changes with increasing molecular concentration. As an example, we show the partial density of states (PDOS) of guanine upon adsorption on graphene at low and high molecular concentrations in Figure 2a. PDOS plots for other nucleobases are available in the Supporting Information (Figures S4−S7). There is a significant shift in all electronic bands from low to high molecular concentrations, particularly in the region near the highest occupied molecular orbital (HOMO) and the lowest unoccupied molecular orbital (LUMO). The energy positions of the HOMO and LUMO are highly molecule-specific for all of the nucleobases, as depicted in Figure 2b, and change with increasing molecular coverage. The overall trend shows an upshift of HOMO and LUMO levels for most of the molecules from low to high molecular concentration, except for adenine, which exhibits a downshift. The shift of HOMO and LUMO levels is on the order of 0.2−0.7 eV from low to high molecular concentration. As each molecular concentration is associated with a different adsorption geometry, these results also provide clear evidence of high sensitivity of the electronic states of the nucleobases to changes in adsorption geometry due to intermolecular interactions. Thus, any fluctuations of the nucleobase adsorption structure on graphene is expected to modify the distinct fingerprints in the electronic density of states (DOS) of the nucleobases,[18,40] causing a complication for their unambiguous identification.

To gain more insights into the origins of distinct electronic structures at low and high molecular concentration, we plot the distribution of charge density difference for guanine in Figure 2c. Similar plots for other nucleobases are shown in Supporting Information (Figures S4−S7). At low molecular concentration, the charge redistribution is concentrated at the interfacial region between aromatic cores of graphene and the nucleobases. In contrast, most of charge redistribution concentrates along the edges of the adsorbed molecules at high molecular concentration. This reinforces the fact that for titled nucleobases at high molecular concentration the graphene−base interaction is not only contributed to by $\pi-\pi$ interaction between aromatic cores but also by the specific side functional groups.

Previous density functional theory calculations of isolated DNA nucleobases adsorbed flat on graphene have identified molecule-induced work function shifts as the dominant mechanism for electronic structure modification of graphene and determination of the doping by the nucleobases.[34] Similar conclusions have been drawn from recent experimental work that measured electronic fingerprints of individual DNA nucleobases deposited on graphene using FETs and X-ray photoelectron spectroscopy (XPS).[32] The measured Dirac point shifts in FETs have followed the same trend as work function shifts determined by XPS, showing a very distinct coverage dependence for each of the DNA nucleobases and providing a new way for their discrimination.[32] Figure 3 shows that the large in-plane dipole moments of DNA/RNA nucleobases (Figure 1a) can significantly alter the work function of graphene (W), particularly when the tilt of the molecules becomes significant. There is a 10-fold increase of the nucleobase-induced work function change of graphene for the tilted high-density nucleobases compared to the isolated flat nucleobases on graphene. Each of the nucleobases causes a very distinct work function change in graphene with increasing molecular density. The work function change in Figure 3 is plotted with respect to the work function of isolated graphene

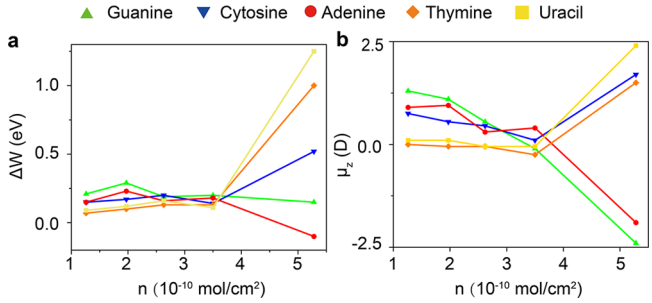

Figure 3. (a) Work function changes of graphene (ΔW) and (b) z-component of molecular dipole moments (μ_z) of adsorbed nucleobases on graphene as a function of molecular concentration for different nucleobases.

(W = 4.25 eV). It is interesting to note that while most of the nucleobases induce p-type doping of graphene (positive work function change), which is consistent with our charge transfer analysis that can be found in Supporting Information (Figure S8), adenine at high coverage induces n-type doping (negative work function change).

The work function changes are found to be closely correlated with the molecular dipole moment of the nucleobases normal to the graphene surface (μ_z) (Figure 3b). Note that positive μ_z refers to the induced dipole moment directed from the nucleobase to graphene. At low molecular concentrations, the z-component of the molecular dipole moments is weak and is predominantly caused by small local structural changes of nucleobases from the flat adsorption geometry (e.g., the pyramidalization of the amino group ($-NH_2$)[51]). μ_z increases significantly at high molecular concentrations as strong intermolecular interactions lead to significant tilt of the nucleobases. These interfacial z-dipole moments act as local electric fields, the strength of which can be estimated as $E = \Delta\Phi/ed$, where $\Delta\Phi$ is the electrostatic potential difference between the vacuum level near the molecule and graphene and d is the separation distance. We find that the tilted molecules at high molecular concentration lead to much higher electric field strength (in the range of 0.21 eV/nm for guanine to 0.56 eV/nm for uracil) compared to that at low molecular concentration (nearly 0.02 eV/nm for all nucleobases). This localized electric field is the main cause of the work function shift. In experiments, the magnitude of this localized field can possibly be estimated using atomic force microscopy techniques as reported in recent studies.[52,53] However, we find that the resulting work function changes deviate significantly from the expected work function changes predicted by the conventional Helmoltz equation, $\Delta W = \mu_z e/\epsilon A$, where A is the area of the graphene supercell.[54−57] Notably, in the case of guanine with a large dipole moment (−2.38 D), we have obtained a small work function increase (0.15 eV), which is in apparent contradiction with the Helmholtz equation. This provides clear evidence of the limited validity of simple electrostatic approximations for weakly adsorbed systems, such as DNA/RNA nucleobases on graphene, and highlights the importance of full quantum mechanical treatment of the problem.

We find that the extent of work function changes caused by adsorption of nucleobases is roughly inversely proportional to the intermolecular binding energy. Guanine has the strongest intermolecular binding energy and also the strongest binding with graphene among all nucleobases at high molecular concentrations. The effect of strong molecular dipole moments

DOI: 10.1021/acs.jpclett.7b01283
J. Phys. Chem. Lett. 2017, 8, 3087−3094

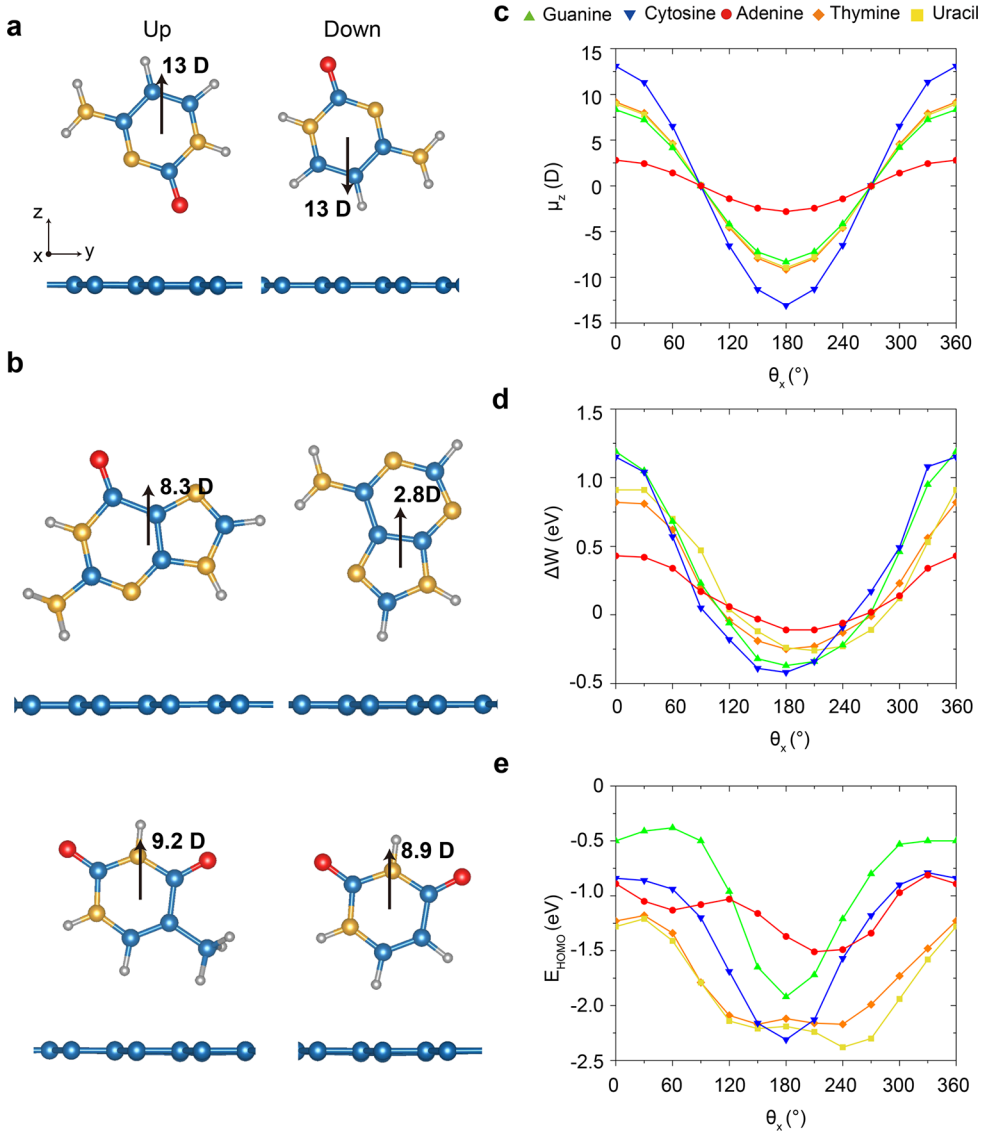

Figure 4. (a) Vertically oriented cytosine adsorbed on graphene with the maximized *z*-component molecule dipole moment (shown in arrows) pointing toward the molecule (denoted as Up) and graphene (denoted as Down). (b) Corresponding Up configurations for guanine, adenine, thymine, and uracil. (c–e) The *z*-component molecular dipole moment μ_z (c), work function changes ΔW (d), and HOMO levels as a function of rotation angle around the *x* axis relative to Up configuration θ_x (e).

of guanine is suppressed by a combined influence of graphene–nulecobase interactions and base–base interactions. Conversely, uracil has a lower intermolecular binding energy (0.24 vs 0.75 eV for guanine) but induces a 1.25 eV work function increase in graphene. These results indicate that the intermolecular interactions and molecular screening effects (e.g., depolarization effect) can significantly lower the effective electric field that originated from molecular dipole moments, particularly at high molecular concentration. The final magnitude of the work function change of graphene at high molecular concentration is a result of a complex interplay between graphene–base and intermolecular interactions, screening effects, and geometry changes of adsorbed molecules on graphene. On the other hand, insights into the competition between graphene–base and intermolecular interactions can also be assessed by calculating the interaction-induced dipole moment (see Table S3 in the Supporting Information), low magnitudes of which show that the interaction between graphene and nucleobase molecules has a smaller effect on the total dipole moment in the molecules.

Close examination of Figures 1–3 reveals that the results presented here can collectively provide key electronic signatures for the type of nucleobase molecule and its concentration. For example, at low concentrations (less than 4×10^{-10} mol/cm^2), the HOMO and LUMO levels provide distinct signals for different nucleobase molecules. On the other hand, at high concentrations, a change in the work function of graphene can effectively distinguish between different types of nucleobases. These observations can be exploited to design nucleobase sensing experiments using graphene as a substrate. These results further motivate us to examine the role of molecular dipoles and are useful for designing effective DNA sequencing experiments using graphene-based electronic devices to maximize measured signals. In DNA sequencing, the contact between graphene and nucleobases is nonplanar and can be off of a low-energy configuration due to the backbone rigidity, temperature, or interactions between

DOI: 10.1021/acs.jpclett.7b01283
J. Phys. Chem. Lett. 2017, 8, 3087–3094

nucleobases and other molecules.[3,58] It has been shown that nucleobases can contact graphene perpendicular to its surface during sequencing.[19,59] Another important aspect is the direction of the dipole moment with respect to the sugar−phosphate group that forms the link between the nucleobase and the backbone. As can be seen in Figure 1a, the direction of the dipole moment (marked by a dashed circle) is completely different for each of the nucleobases; the molecular dipole moment points out for G, C, and A and inward for T and U nucleobases. We next show that the nonplanar adsorption of the nucleobases on graphene, which is typical during DNA/RNA sequencing, has important consequences for the molecular identification.

To simulate experimental conditions, we calculate the changes in the electronic structure upon adsorption of vertically oriented nucleobases at low molecular concentrations. A low molecular concentration is chosen because the distance between the nucleobase in a DNA strand is around 5−7 Å. At these distances, although the noncovalent interactions between neighboring nucleobase interactions are expected to influence the configurational geometry, the effect on the electronic structure can be expected to be minimal.[46,47,60] First, we adjust the molecular geometry of nucleobases so that μ_z of a nucleobase in perpendicular contact with graphene is maximized. We denote the molecular geometry of nucleobases with a large dipole moment directed from graphene to molecule as Up (positive dipole) and the geometry with a large dipole moment directed from graphene to the molecule as Down (negative dipole) (Figure 4a,b). Considering the complexity of the interfacial contact between nucleobases and graphene, we rotate the Up adsorption configuration around the x axis in steps of 30° (the rotation angle is denoted as θ_x). Figure 4c,d shows the magnitude of the molecular dipole moment as a function of the rotation angle and the corresponding work function changes. There is a large difference in work function changes between Up and Down configurations (1−1.6 eV), resulting in p-type and n-type doping of graphene, respectively. It can also be seen that the work function changes in Figure 4d deviate slightly from the sinusoidal trend in Figure 4c; an equal magnitude of molecular dipole moment does not lead to the same magnitude of work function shift. The negative dipole results in much less work function shift compared to the positive molecular dipole. Moreover, the HOMO levels (Figure 4e) of nucleobases also show more asymmetric anisotropic behavior, especially for adenine and uracil. These results can be attributed to the different surface contact between nucleobases and graphene.

In general, a negative molecular dipole moment occurs when an oxygen atom is close to the surface (for adenine, the amino group) (see Supporting Information Table S4 for a summary of all rotational configurations considered). The strong electronegativity of oxygen atoms significantly increases the magnitude of induced molecular dipoles when we compare the molecular dipole of adenine with those of other nucleobases. When θ_x = 90° and 270°, the molecular dipole moment almost vanishes to zero, and we observe only a small work function shift (within 0.1 eV) for all nucleobases. This shows that the molecular dipole is the main driving force for the work function shift rather than the molecule−graphene interactions, consistent with our findings in concentration analysis. However, the strong asymmetric electronic behavior along the molecular rotation proves the strong modulation of the electronegativity difference between the substrate and the adsorbate. Therefore, the final electronic fingerprints of nucleobases on graphene are highly sensitive to the adsorption configuration, resulting in a unique geometry−property correlation for each base, which can be utilized for identification of nucleobases in contact in DNA/RNA sequencing experiments. Moreover, the nucleobase sensing experiments can also take advantage of the behavior of Up and Down molecular dipole moments by using frequency-dependent AC measurements as suggested in some studies.[61] The strong AC field can force the molecule to stand in a perpendicular position to extract a unique electronic signal. This strategy can effectively enhance the measured signals and an ability to distinguish between different nucleobases in molecular sensing schemes. Finally, it should be noted that we have not considered the effect of a substrate on the electronic signatures of nucleobases in graphene. Experiments and theoretical studies have shown that the states of nucleobases can strongly hybridize with the states of the underlying substrate despite the separating layer of graphene.[32,40] This see-through effect is significant near the Fermi level and makes the electronic signals of nucleobases difficult to identify. Consequently, most experiments on nucleobase sensing and sequencing using graphene-based devices are done with a free-standing graphene membrane.[3,23,62,63]

In summary, we have investigated the role of the surface coverage and adsorption geometry on the electronic structure of DNA/RNA nucleobases on graphene using density funtional theory calculations. We have demonstrated that the adsorption behavior of the nucleobases on graphene is determined by a subtle balance between graphene−molecule and intermolecular interactions, where the resulting adsorption geometry and energetics of the system are often decided by the interaction with surrounding molecules. We identify that the in-plane dipole moments play a dominant role in electronic structure modification of graphene with tilted nucleobases on the surface, resulting in both p- and n-type doping of graphene depending on the direction of the z-component of the molecular dipole moment. Moreover, we have found that the electronic fingerprints of nucleobases can be significantly enhanced if the molecular dipoles of nucleobases are appropriately maximized. We observe large differences in work function changes by comparing flat and tilted configurations of nucleobase molecules (up to 1 eV). These results highlight the opportunities to improve the design of current electrochemical sensing devices and provide critical fundamental knowledge for the identification of molecular fingerprints in graphene-based nucleobase sensing and sequencing methods. In addition, this study presents a new perspective on the interaction in a $\pi-\pi$ stacking system from a concentration-dependent view, which challenges the conventional picture of energy band alignment between physisorbed organic molecules and graphene.

■ ASSOCIATED CONTENT

Supporting Information

The Supporting Information is available free of charge on the ACS Publications website at DOI: 10.1021/acs.jpclett.7b01283.

Detailed simulation setup, comparison of different vdW approximations, adsorption distance and rotation angle of nucleobases, PDOS and charge density difference plots for cytosine, adenine, thymine, and uracil, Bader charge transfer plots, and summary of nucleobase surface

DOI: 10.1021/acs.jpclett.7b01283
J. Phys. Chem. Lett. 2017, 8, 3087−3094

contact with graphene when adsorbed vertically oriented (PDF)

AUTHOR INFORMATION

Corresponding Authors

*E-mail: cervenka@fzu.cz (J.C.).

*E-mail: nikhil.medhekar@monash.edu (N.V.M.).

ORCID

Nikhil V. Medhekar: 0000-0003-3124-4430

Notes

The authors declare no competing financial interest.

ACKNOWLEDGMENTS

This research was supported by Australian Research Council's Discovery Project scheme (DE120101100 and DP130102512) as well as the Centre of Excellence in Future Low Energy Electronics (CE170100039). Authors gratefully acknowledge computational support from the Monash Campus Cluster, NCI national facility at the Australian National University and Pawsey Supercomputing facility. J.C. acknowledges financial support of the Czech Science Foundation GACR (Project Number 14-15357S) and the J.E. Purkyne Fellowship of the Czech Academy of Sciences.

REFERENCES

(1) Kuila, T.; Bose, S.; Khanra, P.; Mishra, A. K.; Kim, N. H.; Lee, J. H. Recent Advances in Graphene-based Biosensors. *Biosens. Bioelectron.* **2011**, *26*, 4637−4648.

(2) Shao, Y.; Wang, J.; Wu, H.; Liu, J.; Aksay, I.; Lin, Y. Graphene Based Electrochemical Sensors and Biosensors: A Review. *Electroanalysis* **2010**, *22*, 1027−1036.

(3) Heerema, S. J.; Dekker, C. Graphene Nanodevices for DNA Sequencing. *Nat. Nanotechnol.* **2016**, *11*, 127−136.

(4) Green, N. S.; Norton, M. L. Interactions of DNA with graphene and sensing applications of graphene field-effect transistor devices: A review. *Anal. Chim. Acta* **2015**, *853*, 127−142.

(5) Wu, S.; He, Q.; Tan, C.; Wang, Y.; Zhang, H. Graphene-Based Electrochemical Sensors. *Small* **2013**, *9*, 1160−1172.

(6) Vashist, S. K.; Luong, J. H. Recent Advances in Electrochemical Biosensing Schemes Using Graphene and Graphene-based Nanocomposites. *Carbon* **2015**, *84*, 519−550.

(7) Rodrigo, D.; Limaj, O.; Janner, D.; Etezadi, D.; García de Abajo, F. J.; Pruneri, V.; Altug, H. Mid-infrared Plasmonic Biosensing with graphene. *Science* **2015**, *349*, 165−168.

(8) Dong, H.; Gao, W.; Yan, F.; Ji, H.; Ju, H. Fluorescence Resonance Energy Transfer between Quantum Dots and Graphene Oxide for Sensing Biomolecules. *Anal. Chem.* **2010**, *82*, 5511−5517.

(9) Banerjee, S.; Wilson, J.; Shim, J.; Shankla, M.; Corbin, E. A.; Aksimentiev, A.; Bashir, R. Slowing DNA Transport Using Graphene-DNA Interactions. *Adv. Funct. Mater.* **2015**, *25*, 936−946.

(10) Fu, W.; Feng, L.; Mayer, D.; Panaitov, G.; Kireev, D.; Offenhäusser, A.; Krause, H.-J. Electrolyte-Gated Graphene Ambipolar Frequency Multipliers for Biochemical Sensing. *Nano Lett.* **2016**, *16*, 2295−2300.

(11) Cervenka, J.; Budi, A.; Dontschuk, N.; Stacey, A.; Tadich, A.; Rietwyk, K. J.; Schenk, A.; Edmonds, M. T.; Yin, Y.; Medhekar, N.; et al. Graphene Field Effect Transistor as a Probe of Electronic Structure and Charge Transfer at Organic Molecule-graphene Interfaces. *Nanoscale* **2015**, *7*, 1471−1478.

(12) Yin, Y.; Cervenka, J.; Medhekar, N. V. Tunable Hybridization Between Electronic States of Graphene and Physisorbed Hexacene. *J. Phys. Chem. C* **2015**, *119*, 19526−19534.

(13) Wang, Y.; Li, Z.; Wang, J.; Li, J.; Lin, Y. Graphene and Graphene Oxide: Biofunctionalization and Applications in Biotechnology. *Trends Biotechnol.* **2011**, *29*, 205−212.

(14) Georgakilas, V.; Tiwari, J. N.; Kemp, K. C.; Perman, J. A.; Bourlinos, A. B.; Kim, K. S.; Zboril, R. Noncovalent Functionalization of Graphene and Graphene Oxide for Energy Materials, Biosensing, Catalytic, and Biomedical Applications. *Chem. Rev.* **2016**, *116*, 5464−5519.

(15) Novoselov, K. S.; Geim, A. K.; Morozov, S. V.; Jiang, D.; Zhang, Y.; Dubonos, S. V.; Grigorieva, I. V.; Firsov, A. A. Electric Field Effect in Atomically Thin Carbon Films. *Science* **2004**, *306*, 666−669.

(16) Novoselov, K.; Fal'ko, V.; Colombo, L.; Gellert, P.; Schwab, M.; Kim, K. A Roadmap for Graphene. *Nature* **2012**, *490*, 192−200.

(17) Ferrari, A. C.; Bonaccorso, F.; Fal'Ko, V.; Novoselov, K. S.; Roche, S.; Bøggild, P.; Borini, S.; Koppens, F. H.; Palermo, V.; Pugno, N.; et al. Science and Technology Roadmap for Graphene, Related Two-dimensional Crystals, and Hybrid Systems. *Nanoscale* **2015**, *7*, 4598−4810.

(18) Min, S. K.; Kim, W. Y.; Cho, Y.; Kim, K. S. Fast DNA Sequencing with a Graphene-based Nanochannel Device. *Nat. Nanotechnol.* **2011**, *6*, 162−165.

(19) Traversi, F.; Raillon, C.; Benameur, S.; Liu, K.; Khlybov, S.; Tosun, M.; Krasnozhon, D.; Kis, A.; Radenovic, A. Detecting the Translocation of DNA Through a Nanopore Using Graphene Nanoribbons. *Nat. Nanotechnol.* **2013**, *8*, 939−945.

(20) Schneider, G. F.; Kowalczyk, S. W.; Calado, V. E.; Pandraud, G.; Zandbergen, H. W.; Vandersypen, L. M.; Dekker, C. DNA Translocation Through Graphene Nanopores. *Nano Lett.* **2010**, *10*, 3163−3167.

(21) Freedman, K. J.; Ahn, C. W.; Kim, M. J. Detection of Long and Short DNA Using Nanopores with Graphitic Polyhedral Edges. *ACS Nano* **2013**, *7*, 5008−5016.

(22) Avdoshenko, S. M.; Nozaki, D.; Gomes da Rocha, C.; Gonzalez, J. W.; Lee, M. H.; Gutierrez, R.; Cuniberti, G. Dynamic and Electronic Transport Properties of DNA Translocation Through Graphene Nanopores. *Nano Lett.* **2013**, *13*, 1969−1976.

(23) Postma, H. W. C. Rapid Sequencing of Individual DNA Molecules in Graphene Nanogaps. *Nano Lett.* **2010**, *10*, 420−425.

(24) Nelson, T.; Zhang, B.; Prezhdo, O. V. Detection of Nucleic Acids with Graphene Nanopores: ab initio Characterization of a Novel Sequencing Device. *Nano Lett.* **2010**, *10*, 3237−3242.

(25) Alonso-Cristobal, P.; Vilela, P.; El-Sagheer, A.; Lopez-Cabarcos, E.; Brown, T.; Muskens, O. L.; Rubio-Retama, J.; Kanaras, A. G. Highly Sensitive DNA Sensor Based on Upconversion Nanoparticles and Graphene Oxide. *ACS Appl. Mater. Interfaces* **2015**, *7*, 12422−12429.

(26) Bobadilla, A. D.; Seminario, J. M. Assembly of a Noncovalent DNA Junction on Graphene Sheets and Electron Transport Characteristics. *J. Phys. Chem. C* **2013**, *117*, 26441−26453.

(27) Dong, X.; Shi, Y.; Huang, W.; Chen, P.; Li, L.-J. Electrical Detection of DNA Hybridization with Single-Base Specificity Using Transistors Based on CVD-Grown Graphene Sheets. *Adv. Mater.* **2010**, *22*, 1649−1653.

(28) Huang, Y.; Dong, X.; Shi, Y.; Li, C. M.; Li, L.-J.; Chen, P. Nanoelectronic Biosensors Based on CVD Grown Graphene. *Nanoscale* **2010**, *2*, 1485−1488.

(29) Lin, C.-T.; Loan, P. T. K.; Chen, T.-Y.; Liu, K.-K.; Chen, C.-H.; Wei, K.-H.; Li, L.-J. Label-Free Electrical Detection of DNA Hybridization on Graphene using Hall Effect Measurements: Revisiting the Sensing Mechanism. *Adv. Funct. Mater.* **2013**, *23*, 2301−2307.

(30) Mohanty, N.; Berry, V. Graphene-Based Single-Bacterium Resolution Biodevice and DNA Transistor: Interfacing Graphene Derivatives with Nanoscale and Microscale Biocomponents. *Nano Lett.* **2008**, *8*, 4469−4476.

(31) Lin, J.; Teweldebrhan, D.; Ashraf, K.; Liu, G.; Jing, X.; Yan, Z.; Li, R.; Ozkan, M.; Lake, R. K.; Balandin, A. A.; et al. Gating of Single-Layer Graphene with Single-Stranded Deoxyribonucleic Acids. *Small* **2010**, *6*, 1150−1155.

(32) Dontschuk, N.; Stacey, A.; Tadich, A.; Rietwyk, K. J.; Schenk, A.; Edmonds, M. T.; Shimoni, O.; Pakes, C. I.; Prawer, S.; Cervenka, J.

DOI: 10.1021/acs.jpclett.7b01283
J. Phys. Chem. Lett. 2017, 8, 3087−3094

A Graphene Field-effect Transistor as A Molecule-specific Probe of DNA Nucleobases. *Nat. Commun.* **2015**, *6*, 6563.
(33) Gowtham, S.; Scheicher, R. H.; Ahuja, R.; Pandey, R.; Karna, S. P. Physisorption of Nucleobases on Graphene: Density-functional Calculations. *Phys. Rev. B: Condens. Matter Mater. Phys.* **2007**, *76*, 033401.
(34) Lee, J.-H.; Choi, Y.-K.; Kim, H.-J.; Scheicher, R. H.; Cho, J.-H. Physisorption of DNA Nucleobases on h-BN and Graphene: vdW-corrected DFT Calculations. *J. Phys. Chem. C* **2013**, *117*, 13435−13441.
(35) Varghese, N.; Mogera, U.; Govindaraj, A.; Das, A.; Maiti, P. K.; Sood, A. K.; Rao, C. Binding of DNA nucleobases and Nucleosides with Graphene. *ChemPhysChem* **2009**, *10*, 206−210.
(36) Le, D.; Kara, A.; Schröder, E.; Hyldgaard, P.; Rahman, T. S. Physisorption of Nucleobases on Graphene: A Comparative van der Waals Study. *J. Phys.: Condens. Matter* **2012**, *24*, 424210.
(37) Berland, K.; Chakarova-Käck, S. D.; Cooper, V. R.; Langreth, D. C.; Schröder, E. A van der Waals Density Functional Study of Adenine on Graphene: Single-molecular Adsorption and Overlayer Binding. *J. Phys.: Condens. Matter* **2011**, *23*, 135001.
(38) Antony, J.; Grimme, S. Structures and Interaction Energies of Stacked Graphene−nucleobase Complexes. *Phys. Chem. Chem. Phys.* **2008**, *10*, 2722−2729.
(39) Umadevi, D.; Sastry, G. N. Quantum Mechanical Study of Physisorption of Nucleobases On Carbon Materials: Graphene Versus Carbon Nanotubes. *J. Phys. Chem. Lett.* **2011**, *2*, 1572−1576.
(40) Ahmed, T.; Kilina, S.; Das, T.; Haraldsen, J. T.; Rehr, J. J.; Balatsky, A. V. Electronic Fingerprints of DNA Bases on Graphene. *Nano Lett.* **2012**, *12*, 927−931.
(41) Ahmed, T.; Haraldsen, J. T.; Zhu, J.-X.; Balatsky, A. V. Next-Generation Epigenetic Detection Technique: Identifying Methylated Cytosine Using Graphene Nanopore. *J. Phys. Chem. Lett.* **2014**, *5*, 2601−2607.
(42) Akca, S.; Foroughi, A.; Frochtzwajg, D.; Postma, H. W. C. Competing Interactions in DNA Assembly on Graphene. *PLoS One* **2011**, *6*, e18442.
(43) Perdew, J. P.; Burke, K.; Ernzerhof, M. Generalized Gradient Approximation Made Simple. *Phys. Rev. Lett.* **1996**, *77*, 3865−3868.
(44) Grimme, S. Semiempirical GGA-type density functional constructed with a long-range dispersion correction. *J. Comput. Chem.* **2006**, *27*, 1787−1799.
(45) While experiments show various metastable configurations for the nucleobase molecules at high molecular concentrations (refs 49 and 50), the simulation setup considered here corresponds to the configuration where individual nucleobase molecules are bonded to each other via hydrogen bond monomers. We have verified whether these different configurations significantly alter the electronic structure of the graphene−nucleobase system at high molecular densities. For example, the difference between the work function change upon adsorption of adenine molecules adsorbed in monomer and dimer configurations is within 0.02 eV, whereas the difference in the charge transfer between molecules and graphene is less than 0.003 e^-.
(46) Umadevi, D.; Sastry, G. N. Impact of the Chirality and Curvature of Carbon Nanostructures on Their Interaction with Aromatics and Amino Acids. *ChemPhysChem* **2013**, *14*, 2570−2578.
(47) Umadevi, D.; Panigrahi, S.; Sastry, G. N. Noncovalent Interaction of Carbon Nanostructures. *Acc. Chem. Res.* **2014**, *47*, 2574−2581.
(48) Botti, S.; Rufoloni, A.; Laurenzi, S.; Gay, S.; Rindzevicius, T.; Schmidt, M. S.; Santonicola, M. G. DNA Self-assembly on Graphene Surface Studied by SERS Mapping. *Carbon* **2016**, *109*, 363−372.
(49) Mamdouh, W.; Kelly, R. E. A.; Dong, M.; Kantorovich, L. N.; Besenbacher, F. Two-Dimensional Supramolecular Nanopatterns Formed by the Coadsorption of Guanine and Uracil at the Liquid/Solid Interface. *J. Am. Chem. Soc.* **2008**, *130*, 695−702.
(50) Xu, S.; Dong, M.; Rauls, E.; Otero, R.; Linderoth, T. R.; Besenbacher, F. Coadsorption of Guanine and Cytosine on Graphite: Ordered Structure Based on GC Pairing. *Nano Lett.* **2006**, *6*, 1434−1438.
(51) Šponer, J.; Leszczynski, J.; Hobza, P. Electronic Properties, Hydrogen Bonding, Stacking, and Cation Binding of DNA and RNA Bases. *Biopolymers* **2001**, *61*, 3−31.
(52) Hapala, P.; Švec, M.; Stetsovych, O.; Van Der Heijden, N. J.; Ondráček, M.; Van Der Lit, J.; Mutombo, P.; Swart, I.; Jelínek, P. Mapping the electrostatic force field of single molecules from high-resolution scanning probe images. *Nat. Commun.* **2016**, *7*, 11560.
(53) Ellner, M.; Pavlicek, N.; Pou, P.; Schuler, B.; Moll, N.; Meyer, G.; Gross, L.; Peréz, R. The Electric Field of CO Tips and Its Relevance for Atomic Force Microscopy. *Nano Lett.* **2016**, *16*, 1974−1980.
(54) Monti, O. L. Understanding Interfacial Electronic Structure and Charge Transfer: An Electrostatic Perspective. *J. Phys. Chem. Lett.* **2012**, *3*, 2342−2351.
(55) Leung, T.; Kao, C.; Su, W.; Feng, Y.; Chan, C. Relationship Between Surface Dipole, Work Function and Charge Transfer: Some Exceptions to an Established Rule. *Phys. Rev. B: Condens. Matter Mater. Phys.* **2003**, *68*, 195408.
(56) Hofmann, O. T.; Egger, D. A.; Zojer, E. Work-Function Modification beyond Pinning: When do Molecular Dipoles Count? *Nano Lett.* **2010**, *10*, 4369−4374.
(57) Varene, E.; Bogner, L.; Meyer, S.; Pennec, Y.; Tegeder, P. Coverage-dependent adsorption geometry of octithiophene on Au(111). *Phys. Chem. Chem. Phys.* **2012**, *14*, 691−696.
(58) Deamer, D.; Akeson, M.; Branton, D. Three decades of nanopore sequencing. *Nat. Biotechnol.* **2016**, *34*, 518−524.
(59) Prasongkit, J.; Feliciano, G. T.; Rocha, A. R.; He, Y.; Osotchan, T.; Ahuja, R.; Scheicher, R. H. Theoretical Assessment of Feasibility to Sequence DNA Through Interlayer Electronic Tunneling Transport at Aligned Nanopores in Bilayer Graphene. *Sci. Rep.* **2015**, *5*, 17560.
(60) Prasongkit, J.; Grigoriev, A.; Pathak, B.; Ahuja, R.; Scheicher, R. H. Transverse Conductance of DNA Nucleotides in a Graphene Nanogap from First Principles. *Nano Lett.* **2011**, *11*, 1941−1945.
(61) Rumyantsev, S.; Liu, G.; Shur, M.; Potyrailo, R.; Balandin, A. Selective gas sensing with a single pristine graphene transistor. *Nano Lett.* **2012**, *12*, 2294.
(62) Garaj, S.; Hubbard, W.; Reina, A.; Kong, J.; Branton, D.; Golovchenko, J. Graphene As A Subnanometre Trans-electrode Membrane. *Nature* **2010**, *467*, 190−193.
(63) Arjmandi-Tash, H.; Belyaeva, L. A.; Schneider, G. F. Single molecule detection with graphene and other two-dimensional materials: nanopores and beyond. *Chem. Soc. Rev.* **2016**, *45*, 476−493.

DOI: 10.1021/acs.jpclett.7b01283
J. Phys. Chem. Lett. 2017, 8, 3087−3094